Phys Chem Minerals (2000) 27: 630–637 © Springer-Verlag 2000

ORIGINAL PAPER

S. A. T. Redfern · G. Artioli · R. Rinaldi
C. M. B. Henderson · K. S. Knight · B. J. Wood

Octahedral cation ordering in olivine at high temperature. II: an in situ neutron powder diffraction study on synthetic $MgFeSiO_4$ (Fa50)

Received: 12 August 1999 / Accepted: 25 April 2000

Abstract The partitioning of Fe and Mg between the M1 and M2 octahedral sites of olivine has been investigated by in situ time-of-flight neutron powder diffraction. The degree of M-cation order was determined from direct measurements of site occupancies in a synthetic sample of Fo50Fa50 heated to 1250 °C at the Fe-FeO oxygen buffer. Fe shows slight preference for M1 at temperatures below about 600 °C, progressively disordering on heating to this temperature. Above 630 °C, the temperature at which site preferences cross over (T_{cr}), Fe preferentially occupies M2, becoming progressively more ordered into M2 on increasing temperature. The cation-ordering behaviour is discussed in relation to the temperature dependence of the M1 and M2 site geometries, and it is suggested that vibrational entropy, crystal field effects and changes in bond characteristics play a part in the cross-over of partitioning behaviour. The temperature dependence of site ordering is modelled using a Landau expansion of the free energy of ordering of the type $\Delta G = -hQ + gTQ + \frac{a}{2}(T - T_c)Q^2 + \frac{b}{4}Q^4$, with $a/h = 0.00406\ K^{-1}$, $b/h = 2.3$, $T_c = 572$ K and $g/h = 0.00106\ K^{-1}$. These results suggest that the high-temperature ordering behaviour across the forsterite-fayalite join will have a bearing on the activity-composition relations of this important rock-forming mineral, and indicate that Fe-Mg olivine solid solutions become less ideal as temperature increases.

Key words Olivine · Order/disorder · High temperature cation partitioning · Neutron diffraction (powder)

S. A. T. Redfern (✉)
Department of Earth Sciences, University of Cambridge, Downing Street, Cambridge, CB2 3EQ, UK
e-mail: satr@cam.ac.uk

G. Artioli
Dipartimento di Scienze della Terra, Università di Milano, I-20133 Milano, Italy

R. Rinaldi
Dipartimento di Scienze della Terra, Università di Perugia, I-06100 Perugia, Italy

C. M. B. Henderson
Department of Earth Sciences, University of Manchester, Oxford Road, Manchester, M13 9PL, UK

K. S. Knight
ISIS, Rutherford Appleton Laboratory, Chilton, Didcot, Oxon., OX11 0QX, UK

B. J. Wood
Department of Geology, University of Bristol, Queen's Road, Bristol, BS8 1RJ, UK

Introduction

Natural olivine, M_2SiO_4, where M consists predominantly of Mg and Fe^{2+} plus minor to trace amounts of Ni and other divalent cations, has two non-equivalent octahedral sites M1 (the more distorted) and M2 (the larger), hosting these cations. A knowledge of the effects of composition, temperature and pressure on the non-convergent, intersite ordering/disordering of the octahedral cations is essential for the a thorough understanding of the thermodynamic, petrological and geophysical properties of this phase.

The order/disorder process in olivine is termed non-convergent, since the two M sites over which metal cations may be distributed will always be symmetrically distinct, even if the cations are distributed completely randomly. In this respect it is similar to cation ordering in pyroxenes or spinels. The site occupancies may be related to a distribution coefficient, K_D, for intracrystalline partitioning of the relevant cations over the two sites, where $K_D = [Fe_{M1} \times Mg_{M2}]/[Fe_{M2} \times Mg_{M1}]$ and Fe_{M1} is the atomic fraction of Fe in the M1 site etc. Alternatively, the distribution may be described in terms of an order parameter, Q, describing the degree of cationic order/disorder over the two sites. Since the composition of interest to us in this study is $(Mg_{0.5}Fe_{0.5})_2SiO_4$, the formulation of Q is particularly straightforward:

$$Q = 2[Fe_{M1} - 0.5] \ .$$

Hence, $K_D = 1$ and $Q = 0$ for complete disorder, and Q = 1 or −1 for completely ordered or antiordered states, respectively. This description was used and is described further in the discussion of non-convergent ordering in tephroite-bearing olivines by Redfern et al. (1997).

Several in situ high-temperature neutron diffraction experiments have been carried out on Mg-Fe olivines of different provenance and compositions in the past few years at the single-crystal (SXD: Artioli et al. 1995; Rinaldi et al. 2000) and, more recently, powder (POLARIS) beam lines of the ISIS spallation source (Rutherford Appleton Laboratory, UK). The resulting structure refinements provide a new outlook on the order-disorder dynamics in this important system. Most notably, a peculiar structural response to temperature was revealed, consisting of an unexpected intersite octahedral cation redistribution. Following an initial tendency towards ordering with increasing temperature due to kinetics effects, Fe and Mg undergo an abrupt site exchange, initially reverting towards disorder and then proceeding, through a cross-over temperature, to an almost complete ordering reversal with the onset of an "antiordered" phase which persists up to the highest temperatures within experimental reach. Such structural modifications are effectively not preserved in quenching experiments, owing to the speed of the exchange kinetics.

These results warrant a complete revision of the thermodynamic variables characteristic of olivine also in relation with the coexisting phases in the upper mantle, and a new outlook on the geophysical models involving the olivine-bearing rocks in high-temperature environments. The behaviour of this phase has some bearing also on the much much-debated problems related to the 410-km mantle discontinuity as regards its composition, thickness and physical properties. Recent compressibility studies of forsterite have provided new perspectives on this discontinuity (Duffy et al. 1995; Jeanloz 1995), although these authors do not consider the possible effects of cation partitioning.

In order to resolve the apparent thermodynamical paradox of the degree of order increasing with increasing temperature and the rather unusual phenomenon of ordering reversal that we observe in the Mg-Fe olivine system, several different compositions have been explored and documented. Here, we report the results obtained on synthetic samples of Fo50-Fa50 composition investigated by means of Rietveld structure refinement techniques, which complement experiments on natural single crystals of Fo88 and Fo90 olivines (Rinaldi et al. 2000).

Experimental procedures

Three separate $MgFeSiO_4$ synthetic samples were prepared by grinding together stoichiometric mixtures of Fe_2O_3, MgO and SiO_2 pressed into pellets and crystallized at 1300 °C for three periods of 4 h each, grinding and repelleting in between. The samples were buffered using a CO_2-CO gas mixture at about 1 log unit more oxidizing than the Fe-FeO buffer and were quenched within the reducing gas atmosphere to below 500 °C in less than 1 min. X-ray powder diffraction showed all batches to be phase-pure, with sharp peaks indicating good crystallinity and homogeneity. Electron microprobe analysis at Manchester University (Cameca Camebax WDS) showed the samples to be homogeneous and stoichiometric within experimental error ($Mg_{0.500}$-$Mg_{0.504}$).

Neutron diffraction data were obtained at the Polaris time-of-flight diffractometer of the ISIS neutron spallation source (Hull et al. 1992). The instrument allows collection of data across the wide range of scattering vectors necessary for discriminating site occupancies and displacement factors to high precision, with low errors (1–2%) in the determination of K_D values. Cell dimensions are also determined with high precision, typically to 1 part in 70 000. A fixed scattering geometry and a relatively high flux at the detector with low background characterize this instrument, which allows rapid data collection from large thermally stable samples that can be heated to extreme temperatures (up to 2000 °C at ISIS) with fO_2 buffering, if needed.

Experiments were carried out at different times under slightly different operating conditions and with different samples. In the first run, the sample (3.5–4 g) was loaded into a thin-walled silica glass tube separated from a Fe-FeO buffer by silica glass wool and evacuated to a residual pressure of 5×10^{-7} mbar inside the furnace assembly. In a subsequent experiment, a better sample presentation consisting of sintered pellets held in a tantalum wire wire-mesh basket allowed us to reach slightly higher temperatures. We saw no evidence of oxidation of any of our samples, even at the highest temperatures of measurement. This is not surprising considering the high-vacuum conditions of the experiment, the presence of an Fe-FeO buffer next to the sample and the close proximity of vanadium (and tantalum) to the sample, which acts as an efficient oxygen getter.

The data from individual detectors were corrected for electronic noise, normalized against standard spectra from a sample of vanadium, and focused using in-house software. No corrections were made for beam attenuation by the furnace or sample, since these were found to be negligible. The data used in the structure refinements were from the "C" backscattering bank of detectors, covering the 2θ range between 130° and 160°. The powder histograms were collected from 2.98 to 19.60 ms (corresponding to a d spacing range between 0.48 and 3.17 Å) and were rebinned to a total of 1875 data points per histogram. The experimental arrangements are detailed in Table 1.

The crystal structures were refined using the GSAS Rietveld refinement software (Larson and Von Dreele 1994). The results of a typical refinement are shown in Fig. 1. High-temperature structural data were obtained by Rietveld refinement of neutron powder diffraction data sets collected over periods of about 2 h each within the heating and cooling cycles up to the experimental limit of 1250 °C typical of the vanadium furnace employed.

Results and discussion

Results from the synthetic Fa50 olivines [$(Mg_{0.5}Fe_{0.5})_2SiO_4$] were analyzed in detail in terms of variations induced by temperature on the most significant crystallographic parameters such as unit cell dimensions, M-site occupancies and distributions of the two octahedral species (Mg and Fe), atomic displacement parameters of M1 and M2 sites, octahedral volumes of the two sites and M1-O and M2-O individual distances. Results are summarized in Tables 2 and 3.

The octahedral occupancies were refined by imposing full site occupancy of each site (i.e. $Fe_{M1} + Mg_{M1} = 1.0$; $Fe_{M2} + Mg_{M2} = 1.0$) and assuming nominal stoichiometry (i.e. Fe/Mg = 1.0). Under these assumptions the

Table 1 Experimental and instrumental parameters pertaining to the Rietveld refinements

Instrumental	
Diffractometer	POLARIS (neutron time-of-flight powder diffractometer)
Flight path	12.7837 m
Detector	38 ^{3}He gas tubes, 145° 2θ
Data range	2980.00–19600.00 μs
Time channel binning	$dt/t = 5 \times 10^{-3}$
Temperature	See Table 2
Refinement	
Space group	*Pbnm*
Z	4
Unit cell refinement	Whole pattern
Observations	1875
Refined parameters	
Structural	18
Profile	5
Background	12 Chebychev polynomials of the first kind
Cell	3
Constraints	
Strict (equal U_{iso})	Fe1 = Mg1, Fe2 = Mg2
Strict (Σsite = 1)	Fe1 + Mg1, Fe2 + Mg2, Fe1 + Fe2, Mg1 + Mg2
Thermal parameters	All atoms isotropic
Agreement factors	See Table 2

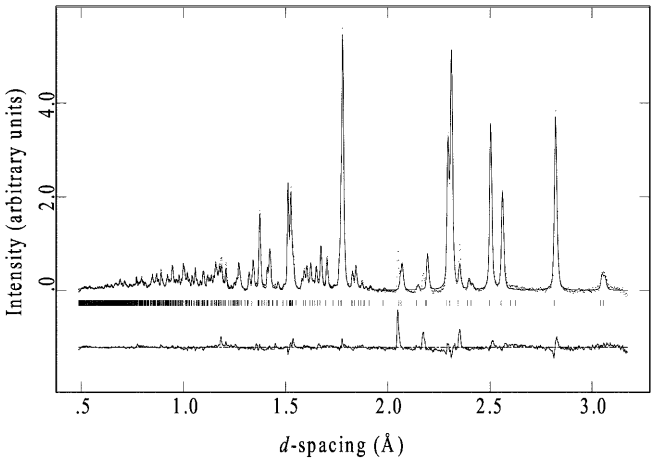

Fig. 1 Comparison of the experimental (*dots*) and calculated (*solid line*) neutron powder diffraction pattern for $MgFeSiO_4$ olivine at 600 °C, together with the difference plot (*below*) and expected peak positions (*tick marks*). The three peaks between 2.0 and 2.5 Å arise from the Vanadium furnace element

atomic coordinates, site occupancy factors and isotropic atomic displacement parameters listed in Table 2 were refined simultaneously. No significant parameter correlation was found during the least-squares minimization. The largest coefficients in the correlation matrix were below 0.70.

The cell parameters are given as a function of temperature in Fig. 2, showing the smooth increase throughout the temperature range over which we have measured ordering. The main feature of interest is, of course, the degree of partitioning of Mg and Fe between the two octahedral sites, shown as K_D vs. T in Fig. 3.

All of our quenched synthetic samples show values of K_D at room temperature that are slightly greater than 1, indicative of a slight preference of Fe^{2+} for the M1 site. On heating, the degree of order decreases (as is expected at a for non-convergent order-disorder processes), falling to zero ($K_D = 1$) at around 650 °C (Fig. 3). Disordering begins to take place at around 300 to 400 °C, with the initial degree of order measured corresponding to that frozen in on quenching in the synthesis procedure. From these values it is clear that the kinetics of Mg-Fe ordering and disordering in olivine are faster than those of Mg-Mn and Fe-Mn order-disorder earlier

Table 2 Structural data for Fo50Fa50 as a function of temperature from the two experiments, refined in space group *Pbnm*

T (°C)	Six	Siy	$U_{iso} \times 100$	O1x	O1y	$U_{iso} \times 100$	O2x	O2y	$U_{iso} \times 100$	O3x	O3y
100	0.4253(8)	0.0977(4)	0.247(57)	0.7683(9)	0.0915(4)	1.124(74)	0.2172(8)	0.4510(3)	0.681(65)	0.2826(5)	0.1641(3)
200	0.4251(8)	0.0977(5)	0.356(62)	0.7680(9)	0.0918(4)	1.309(82)	0.2174(8)	0.4515(3)	0.826(70)	0.2826(5)	0.1640(3)
300	0.4252(8)	0.0975(5)	0.456(66)	0.7680(9)	0.0923(4)	1.462(88)	0.2172(9)	0.4519(4)	0.964(75)	0.2827(6)	0.1638(3)
350	0.4250(9)	0.0974(5)	0.524(69)	0.7676(9)	0.0924(4)	1.533(91)	0.2169(9)	0.4521(4)	1.023(77)	0.2827(6)	0.1637(3)
400	0.4248(9)	0.0973(5)	0.586(73)	0.7678(10)	0.0924(5)	1.664(97)	0.2174(9)	0.4522(4)	1.118(81)	0.2827(6)	0.1636(3)
450	0.4246(9)	0.0972(5)	0.623(75)	0.7678(10)	0.0922(5)	1.76(10)	0.2174(9)	0.4522(4)	1.149(83)	0.2826(6)	0.1633(3)
500	0.4245(9)	0.0973(5)	0.667(78)	0.7679(10)	0.0919(5)	1.89(11)	0.2177(9)	0.4523(4)	1.211(86)	0.2826(6)	0.1633(3)
550	0.4242(9)	0.0973(5)	0.741(81)	0.7675(10)	0.0917(5)	2.02(11)	0.2175(9)	0.4524(4)	1.295(88)	0.2826(6)	0.1631(3)
600	0.4240(10)	0.0974(5)	0.821(85)	0.7682(10)	0.0913(5)	2.11(11)	0.2175(10)	0.4526(4)	1.402(93)	0.2824(6)	0.1629(3)
700	0.4234(10)	0.0974(5)	0.958(90)	0.7680(10)	0.0918(5)	2.17(12)	0.2168(10)	0.4529(4)	1.623(98)	0.2827(6)	0.1627(3)
800	0.4224(10)	0.0983(5)	1.137(94)	0.7661(10)	0.0932(5)	2.39(12)	0.2147(10)	0.4530(5)	2.01(11)	0.2838(6)	0.1624(3)
850	0.4221(10)	0.0985(5)	1.201(98)	0.7658(10)	0.0933(5)	2.45(12)	0.2142(10)	0.4532(5)	2.17(11)	0.2839(6)	0.1625(3)
900	0.4217(10)	0.0988(6)	1.31(11)	0.7655(10)	0.0933(5)	2.59(13)	0.2139(10)	0.4535(5)	2.29(12)	0.2837(6)	0.1625(3)
1050	0.4205(15)	0.0958(8)	1.65(16)	0.7677(15)	0.0953(7)	2.30(17)	0.2211(14)	0.4537(7)	2.60(17)	0.2861(9)	0.1650(5)
1150	0.4203(15)	0.0959(8)	1.80(16)	0.7676(14)	0.0954(7)	2.42(17)	0.2214(14)	0.4540(7)	2.83(18)	0.2861(9)	0.1652(5)
1200	0.4202(15)	0.0960(8)	1.86(16)	0.7666(14)	0.0957(7)	2.39(17)	0.2207(14)	0.4543(7)	2.89(17)	0.2859(9)	0.1653(5)
1225	0.4210(15)	0.0955(8)	1.84(16)	0.7663(14)	0.0961(6)	2.30(16)	0.2211(14)	0.4541(7)	2.92(17)	0.2855(9)	0.1654(5)
1250	0.4209(15)	0.0954(8)	1.83(16)	0.7672(14)	0.0967(6)	2.19(16)	0.2211(14)	0.4540(7)	2.98(18)	0.2857(9)	0.1658(5)

Only the free positional parameters are shown: in addition O1z = O2z = M2z = Siz = 1/4, M1x = M1y = M1z = 0. The Fe content of M1, X_{Fe}^{M1}, is given. Note that $X_{Fe}^{M1} = X_{Mg}^{M2} = 1 - X_{Mg}^{M1} = 1 - X_{Fe}^{M1}$. *Numbers in parentheses* are the calculated standard errors

measured by Redfern et al. (1996, 1997). Upon further heating, the site preferences appear to reverse and Fe^{2+} preferentially enters M2, with K_D passing decreasing below 1. In other words, we find that the crystal orders upon increasing temperature. We term the temperature at which site preferences reverse the ''cross-over temperature'' between ordered and antiordered states, T_{cr}. The Fe^{2+} site preference is for M1 below T_{cr} and for M2 above T_{cr}. The onset of the high-temperature ordering reversal is followed by a strong preference of Fe^{2+} for site M2, reaching a maximum site concentration of some 66% at the maximum temperature reached in the experiment (1250 °C). This is a significant degree of antiorder, noteworthy because the degree of antiorder is increases with increasing temperature. A comparison with the results obtained on the natural olivine ($(Mg_{0.88}Fe_{0.12})_2SiO_4$ from the Brenham pallasitic meteorite (Artioli et al. 1995; Rinaldi et al. 2000)) suggests that the cross-over temperature may be a function of chemical composition, with T_{cr} increasing with increasing Mg content.

Turning to the temperature dependence of the detailed structure, and its relationship to the ordering behaviour, we now consider the bond lengths at the M1 and M2 octahedra. The relative thermal expansion of these sites, $\alpha_{(M1)}$ and $\alpha_{(M2)}$, reverses at T_{cr}, with $\alpha_{(M1)} > \alpha_{(M2)}$ above T_{cr} and $\alpha_{(M1)} < \alpha_{(M2)}$ below T_{cr} (Fig. 4). This would appear to contradict expectations based simply on ionic size considerations. In fact, although the ionic radius of Fe^{2+} is larger than that of Mg^{2+}, as the temperature is raised above T_{cr}, the increase of Fe^{2+} in M2 reduces the rate of expansion of the M2 octahedron and increases the rate of expansion of the M1 octahedron as its Mg occupancy increases. In other words, it seems that the thermal expansion of the Fe-O bond in either M1 or M2 is smaller than that of the Mg-O bond, and the details of the individual site expansions reflect the changes in occupancy.

On inspection of the individual M-O bond lengths at M1 and M2, it becomes clear that the M-O1 bonds play a significant part in controlling the geometry of the octahedra (Fig. 5). The M1-O1 and M2-O1 bond lengths show complementary temperature dependence. M1-O1 is relatively constant below T_{cr}, followed by an increase at higher temperatures, and while M2-O1 increases on heating to T_{cr}, but then decreases once more above T_{cr}. These effects are reflected in the individual M1 and M2 octahedral volumes, and show up most clearly on the (M2-O1)-(M1-O1) plot (Fig. 5b). The O1 oxygen is bonded to four atoms in the structure: two M1 cations, one M2 cation and an adjoining tetrahedral Si. The M1 cations form an octahedral chain, with the M2 octahedra in staggered alternate positions on either side of this chain. The O1 oxygen therefore resides at a pivotal position and appears to accommodate the local strains due to both site exchange and thermal expansion. The temperature dependence of the difference in M-O1 bond lengths shows certain similarities to the relaxation effects seen on the initiation of cation exchange during disordering of Mn-Mg and Mn-Fe olivines (Redfern et al. 1997). This could imply that the M-O1 bond-length difference is a sensitive structural measure of the high-temperature order-disorder behaviour, suggesting that similar relaxation in Fo50Fa50 may be taking place at or around T_{cr}.

The compensating behaviour between the rates of thermal expansion of the two octahedral volumes is responsible for the cancelling out of any effects that the temperature variation of site occupancy may have on the cell parameters (Fig. 2) and volume. The unit cell is thus effectively independent of site occupancy. The inverse relationship between $\alpha_{(M1)}$ and $\alpha_{(M2)}$ also suggests that

Table 2 (continued)

O3z	$U_{iso} \times 100$	Fe(M1)	$U_{iso} \times 100$	M2x	M2y	$U_{iso} \times 100$	a (Å)	b (Å)	c (Å)	K_D	R_{wp}%
0.0348(4)	0.738(45)	0.537(17)	0.793(53)	0.9919(8)	0.2787(3)	0.532(56)	4.8025(3)	10.3648(5)	6.0529(3)	1.35(12)	3.25
0.0348(4)	0.847(49)	0.537(18)	0.967(58)	0.9918(9)	0.2788(3)	0.719(63)	4.8065(2)	10.3759(4)	6.0609(2)	1.35(13)	3.19
0.0351(5)	0.962(53)	0.530(18)	1.136(64)	0.9925(9)	0.2787(3)	0.876(68)	4.8106(2)	10.3863(4)	6.0682(2)	1.27(12)	3.14
0.0353(5)	0.997(54)	0.525(18)	1.187(66)	0.9922(9)	0.2785(3)	0.962(71)	4.8126(2)	10.3916(4)	6.0721(2)	1.22(12)	3.24
0.0353(5)	1.068(57)	0.514(19)	1.264(70)	0.9923(10)	0.2785(3)	1.062(75)	4.8147(2)	10.3971(4)	6.0760(2)	1.12(12)	3.26
0.0354(5)	1.172(59)	0.515(19)	1.354(73)	0.9917(10)	0.2787(3)	1.127(80)	4.8168(2)	10.4029(4)	6.0800(2)	1.13(12)	3.13
0.0355(5)	1.221(61)	0.518(19)	1.450(77)	0.9919(10)	0.2787(3)	1.203(82)	4.8190(2)	10.4091(3)	6.0841(2)	1.15(15)	3.08
0.0354(5)	1.317(64)	0.515(19)	1.573(81)	0.9919(10)	0.2787(3)	1.273(85)	4.8212(2)	10.4148(3)	6.0882(2)	1.13(13)	3.07
0.0355(5)	1.384(66)	0.506(20)	1.608(84)	0.9913(10)	0.2790(3)	1.395(90)	4.8233(2)	10.4211(4)	6.0923(2)	1.05(12)	2.93
0.0356(6)	1.546(70)	0.484(20)	1.714(88)	0.9912(10)	0.2793(3)	1.678(97)	4.8276(2)	10.4332(4)	6.1001(2)	0.88(10)	2.84
0.0353(6)	1.726(72)	0.460(19)	1.801(90)	0.9906(10)	0.2793(3)	2.03(10)	4.8321(2)	10.4453(4)	6.1078(2)	0.73(8)	2.55
0.0354(6)	1.856(77)	0.449(20)	1.864(95)	0.9902(11)	0.2792(3)	2.18(11)	4.8341(2)	10.4515(4)	6.1115(2)	0.66(8)	2.64
0.0355(6)	1.972(82)	0.443(20)	1.94(10)	0.9896(11)	0.2792(4)	2.33(12)	4.8363(2)	10.4582(4)	6.1155(2)	0.63(8)	2.74
0.0387(8)	2.12(12)	0.449(27)	1.77(13)	0.9798(14)	0.2815(5)	2.67(17)	4.8426(2)	10.4810(4)	6.1284(2)	0.66(11)	5.82
0.0392(8)	2.38(12)	0.436(27)	1.96(14)	0.9794(14)	0.2819(5)	3.01(18)	4.8472(2)	10.4955(4)	6.1368(2)	0.60(10)	5.24
0.0395(8)	2.49(12)	0.420(27)	2.02(14)	0.9786(14)	0.2817(5)	3.17(18)	4.8488(2)	10.5009(4)	6.1399(2)	0.52(10)	4.93
0.0395(8)	2.48(12)	0.418(26)	2.00(14)	0.9781(14)	0.2817(5)	3.17(18)	4.8494(2)	10.5023(4)	6.1409(2)	0.52(9)	4.72
0.0399(8)	2.52(13)	0.420(27)	2.01(14)	0.9764(14)	0.2818(5)	3.27(19)	4.8497(2)	10.5034(4)	6.1418(2)	0.52(10)	4.95

Table 3 Temperature dependence of the bond lengths, in Å, for the metal-oxygen bonds at the M1 and M2 sites of Fo50Fa50. *Figures in parentheses* are the calculated standard errors

T (0 °C)	M1-O1	M1-O2	M1-O3	M2-O1	M2-O2	M2-O3a	M2-O3b
100	2.104 (3)	2.096 (3)	2.186 (3)	2.218 (6)	2.088 (5)	2.248 (4)	2.082 (3)
200	2.109 (3)	2.096 (3)	2.187 (3)	2.219 (6)	2.094 (6)	2.253 (4)	2.084 (3)
300	2.113 (3)	2.098 (3)	2.188 (3)	2.217 (6)	2.098 (6)	2.253 (4)	2.090 (3)
350	2.116 (3)	2.100 (3)	2.189 (3)	2.216 (6)	2.103 (6)	2.253 (4)	2.092 (3)
400	2.117 (3)	2.099 (3)	2.189 (3)	2.217 (7)	2.106 (6)	2.255 (4)	2.094 (3)
450	2.117 (4)	2.100 (3)	2.188 (3)	2.219 (7)	2.108 (6)	2.260 (4)	2.095 (3)
500	2.117 (4)	2.100 (3)	2.189 (3)	2.224 (7)	2.109 (6)	2.260 (4)	2.097 (4)
550	2.118 (4)	2.102 (3)	2.188 (3)	2.228 (7)	2.111 (6)	2.263 (4)	2.099 (4)
600	2.116 (4)	2.103 (3)	2.188 (3)	2.233 (7)	2.113 (7)	2.268 (5)	2.099 (4)
700	2.121 (4)	2.106 (3)	2.189 (3)	2.233 (7)	2.114 (7)	2.274 (5)	2.101 (4)
800	2.135 (4)	2.115 (3)	2.192 (3)	2.226 (7)	2.113 (7)	2.285 (5)	2.099 (4)
850	2.137 (4)	2.117 (3)	2.195 (3)	2.225 (8)	2.117 (7)	2.285 (5)	2.099 (4)
900	2.139 (4)	2.119 (4)	2.195 (4)	2.226 (8)	2.121 (7)	2.287 (5)	2.101 (4)
1050	2.147 (5)	2.099 (5)	2.229 (5)	2.205 (10)	2.151 (10)	2.317 (7)	2.080 (5)
1150	2.151 (5)	2.100 (5)	2.233 (5)	2.209 (10)	2.154 (10)	2.320 (7)	2.082 (5)
1200	2.156 (5)	2.103 (5)	2.235 (5)	2.207 (10)	2.159 (10)	2.321 (7)	2.084 (5)
1225	2.158 (5)	2.102 (5)	2.234 (5)	2.203 (10)	2.160 (10)	2.321 (7)	2.084 (5)
1250	2.159 (5))	2.102 (5)	2.238 (5)	2.194 (10)	2.163 (10)	2.324 (7)	2.080 (5)

the much lower thermal expansion coefficient of the Fe-O bond, when compared with that of the Mg-O bond, might be due to a higher degree of covalency of the Fe-O bond at these temperatures. A model of Fe^{2+} partitioning in olivine regulated by the two opposing controls of ionic size and degree of covalent bonding was postulated by Ghose (1981), and our results seem to support this hypothesis. Furthermore, our crystal-chemical observations provide important insights for a better definition of the fundamental crystallographic and thermodynamic parameters of olivine.

By the same token, one may infer that, although marred by a much lower degree of accuracy, intrinsic to the data collection method, the cell-dimension variations observed by Rinaldi and Wilson (1996) and Rinaldi et al. (2000) on single crystals of Fa12 compositions may actually reflect the octahedral volume changes induced by the thermal treatment and the ensuing cation exchange.

We can also consider the thermal expansion of the two octahedral sites merely in terms of geometric effects induced by the two different kinds of octahedral configurations and the implications on the cations' redistribution. Similar effects have been invoked in the case of amphiboles (Oberti et al. 1995). Whatever the origin of the effect seen in Fig. 3, it is clear that there must be some structural control on the relative energetics of Fe and Mg in M1 and M2 that is dependent upon temperature, such that preferences reverse at T_{cr}.

As well as the behaviour of the site occupancies, the atomic displacement parameters also show a cross-over at T_{cr}, diverging above this temperature, with U_{iso}(M2) consistently higher than U_{iso}(M1) as shown in Fig. 6. This reinforces the hypothesis that the increase of the vibrational contribution to entropy overrides the decrease of the configurational contribution as temperature increases. Thus, the unusual thermal behaviour of increasing configurational order with increasing temperature may be interpreted in terms of the total free energy, as postulated earlier by Artioli et al. (1995) and lastly confirmed by Rinaldi et al. (2000). The vibrational characteristics of the two sites may also affect the chemical potentials of these sites, through coupling between crystal field stabilization and M-site vibrational modes. Walsh et al. (1974) first indicated that the effects of vibration-induced Jahn-Teller stabilization at the M2 site may be significant in olivine. Since this site is a quasitrigonally distorted octahedron, a dynamic Jahn-Teller interaction results in additional stabilization of Fe^{2+} in this site over Fe^{2+} in M1 (which is quasitetragonally distorted, and hence has no dynamic Jahn-Teller contribution). The magnitude of this Jahn-Teller interaction can be expected to increase as the amplitude of the vibration at the site increases. Thus, with increasing temperature, we might anticipate that Fe^{2+} would show an increasing preference for M2 due to the increasing crystal field stabilization of this site, resulting in the observed antiordering with temperature.

Thermodynamics of Fe-Mg order/disorder

The magnitude of the intersite M1-M2 exchange energy may be estimated from our site-partitioning data using the Van't Hoff equation, relating $\ln K_D$ to inverse temperature. We find, applying this method to all our data for temperatures above 750 K, a value for the intersite exchange energy of Mg-Fe exchange of 11.1 ± 1.5 kJ mol^{-1}. This compares with values obtained by Henderson et al. (1996) for Mg-Mn exchange and Fe-Mn exchange of 15.7 ± 0.9 and 10.1 ± 0.3 kJ mol^{-1}, respectively.

The thermodynamics of the non-configurational disordering of Fe-Mn and Mg-Mn olivines was described by Redfern et al. (1996, 1997), using a Landau expres-

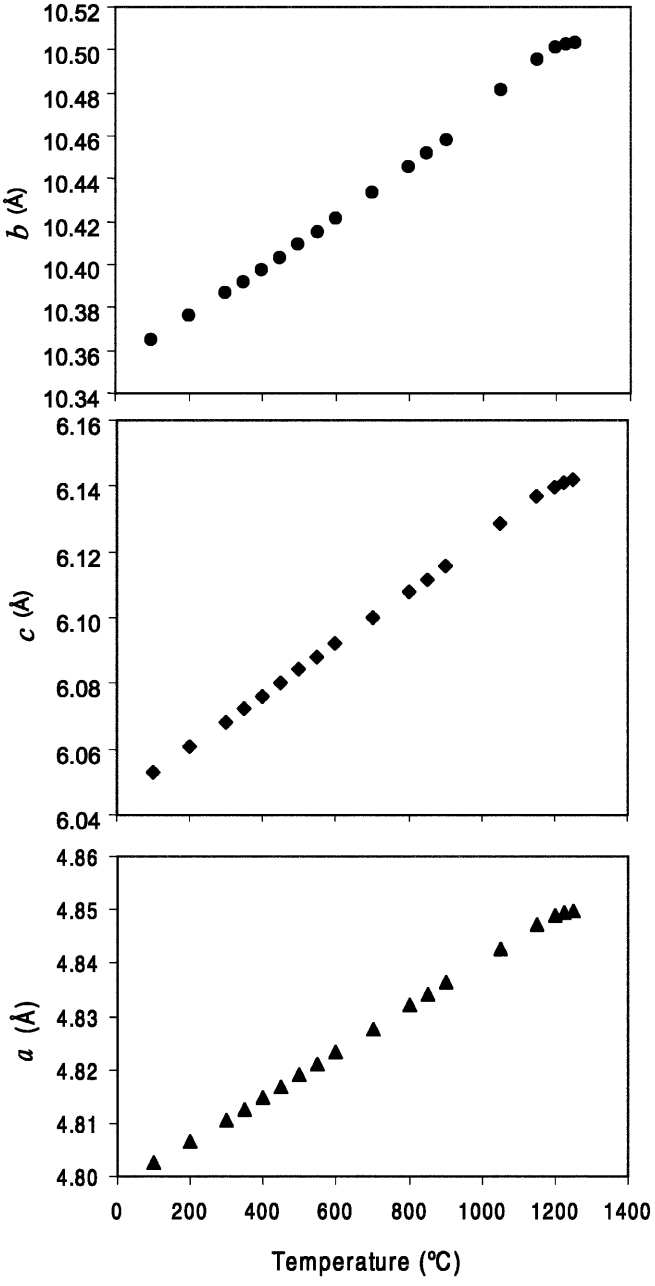

Fig. 2 Temperature dependence of the unit cell parameters of $(Mg_{0.5}Fe_{0.5})_2SiO_4$

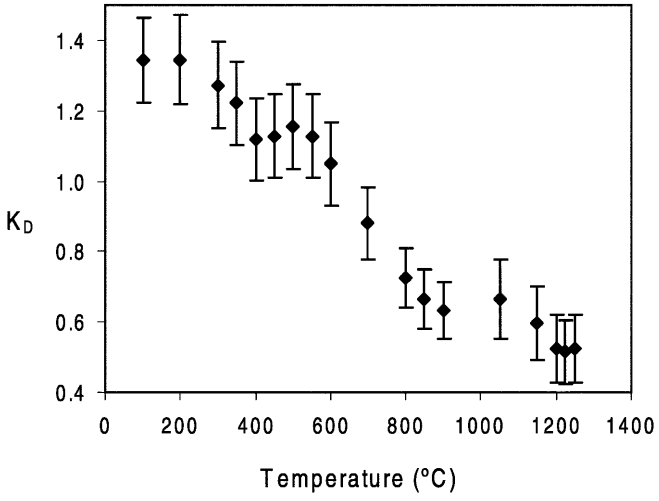

Fig. 3 K_D vs. temperature for Fo50. Below 500 °C the samples are essentially Fe/Mg disordered, with Fe showing a slight preference for M1, but at higher temperatures (from about 650 °C) cations reverse their order, showing preference for the opposite octahedral sites

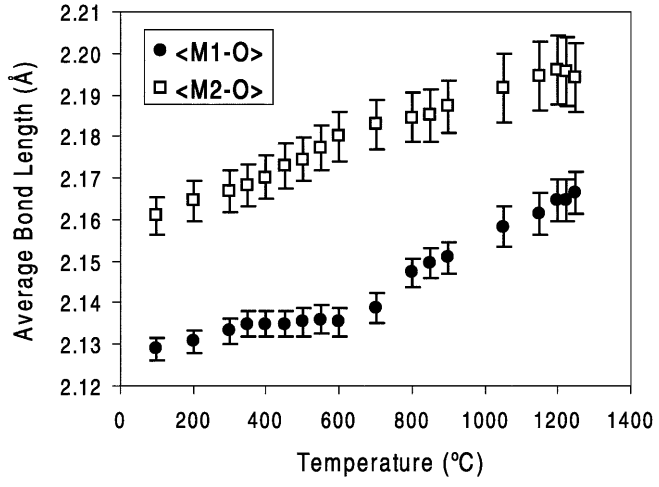

Fig. 4 Temperature dependence of the average bond lengths to oxygen at the M1 and M2 sites. The behaviour above and below about 630 °C (T_{cr}) shows different trends

sion for the equilibrium free energy due to ordering, ΔG, given by:

$$\Delta G = -hQ + \frac{a}{2}(T - T_c)Q^2 + \frac{b}{4}Q^4 \ ,$$

where T_c, h, a and b are material-dependent parameters. The equilibrium temperature dependence of the order parameter, Q, is given by the condition $\partial(\Delta G)/\partial Q = 0$. This model for the free energy does not, however, extend to the description of the unusual order to anti-order behaviour we have observed in Fe-Mg olivines, since it describes ordering that converges asymptotically to zero from a positive value of Q on heating. To take account of the stability of the antiordered state at higher temperatures, we need to add another temperature-dependent (entropy) term to the expression for free energy, so that the excess entropy is described as $\Delta S = -\frac{a}{2}Q^2 - gQ$, and hence the excess free energy becomes:

$$\Delta G = -hQ + gTQ + \frac{a}{2}(T - T_c)Q^2 + \frac{b}{4}Q^4 \ .$$

If we now add the condition that $Q = 1$ at $T = 0$ K and employ the condition $\partial(\Delta G)/\partial Q = 0$, we arrive at a fit to the data shown by Fig. 6 (inset), with the parameters $a/h = 0.00406\ K^{-1}$, $b/h = 2.3$, $T_c = 572$ K and $g/h = 0.00106\ K^{-1}$. These compare with values for a/h of 0.00656 and $0.00523\ K^{-1}$ for $MgMnSiO_4$ and $FeMnSiO_4$, respectively, values of b/h of 10.9 and 13.4

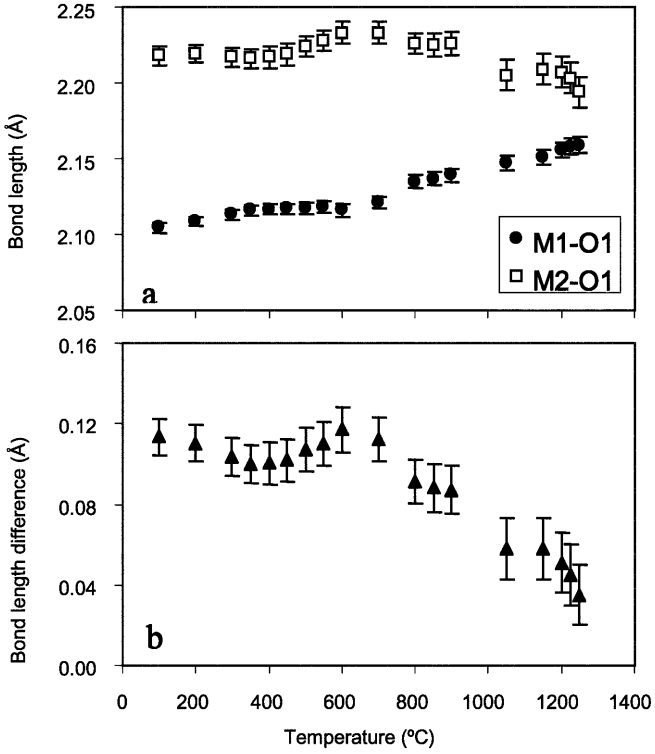

Fig. 5 **a** Temperature dependence of the M-O1 bond lengths. Both M1-O1 and M2-O1 show anomalous behaviour near T_{cr}, with the former decreasing as the latter increases, followed by the opposite trend above T_{cr}. **b** Difference between the M1-O1 and M2-O2 bond lengths, showing that these bonds approach the same length at high temperatures

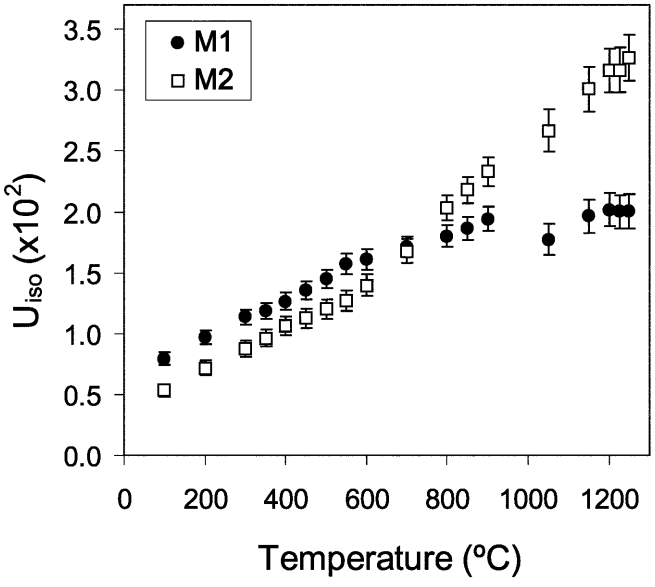

Fig. 6 Atomic displacement parameters of the M1 sites (*filled circles*) and M2 sites (*open squares*) as a function of temperature in Fo50, showing the cross-over of U_{iso} at T_{cr}

for $MgMnSiO_4$ and $FeMnSiO_4$, respectively, and values of T_c of 874 and 645 K for $MgMnSiO_4$ and $FeMnSiO_4$, respectively.

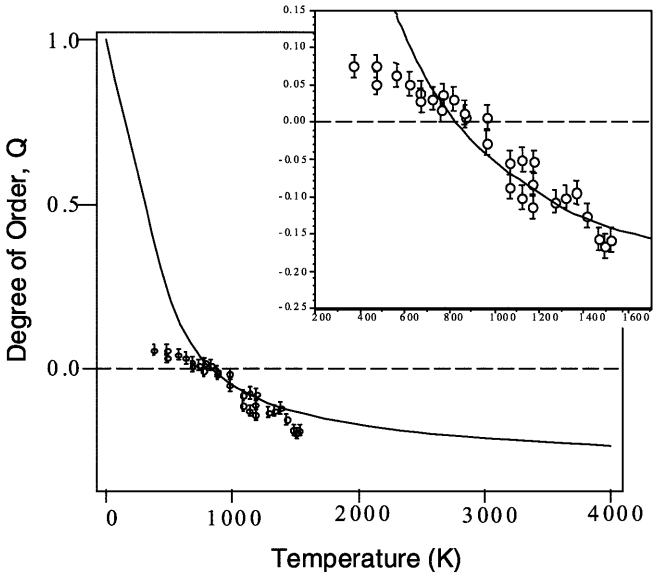

Fig. 7 Landau model for the non-convergent ordering in Fo50Fa50, incorporating the change from order to antiorder. The *inset* shows the fit over the range of the experimental data, suggesting that the data below around 800 K are not in equilibrium

The additional entropy term, linear in Q, is equivalent to the extra vibrational contribution invoked to explain the increasing antiorder with increasing temperature. We see from Fig. 7 that, in this model, the order saturates at some negative value of Q at high temperatures. Indeed, the prediction is that, up to the melting point, olivine will continue to show significant configurational antiorder.

Conclusions

The results we have obtained in this study, using powder neutron diffraction, support the findings of all previous single-crystal Laue neutron diffraction studies of Artioli et al. (1995), Rinaldi and Wilson (1996) and Rinaldi et al. (2000), confirming the unusual temperature-dependent reversal in site preferences for Fe and Mg on the M1 and M2 octahedral sites of olivines. The study described here gives accurate site occupancies, with lower errors than has been possible in previous work, for sample studies during in situ heating in the presence of an fo_2 buffer. These powder data also give higher precision cell parameters than the single-crystal studies, allowing us to infer the detailed changes in site geometries that accompany the reversal in site occupancies. Furthermore, this study extends the composition range over which this behaviour has been observed, showing that the temperature at which the reversal from order to antiorder occurs is strongly composition-dependent. This, in itself, suggests that the high-temperature ordering behaviour across the forsterite-fayalite join will have a bearing on the activity-composition relations of this important rock-

forming mineral. Our results indicate that Fe-Mg olivine solid solutions become less ideal as temperature increases.

Acknowledgements Neutron beam time, awarded by CLRC, was funded by the NERC, the Italian CNR and the Large-Scale Facilities Programme of the EU. Financial support from CNR (grant to RR) and MURST (Progetto biennale cofinanziato 1997, Project Relazioni tra struttura e proprietà dei minerali: analisi ed applicazioni) is acknowledged. Helpful discussion with Subrata Ghose on the behaviour of Fe in olivine is acknowledged by R.R.

References

Artioli G, Rinaldi R, Wilson CC, Zanazzi PF (1995) High-temperature Fe-Mg cation partitioning in olivine: in-situ single-crystal neutron diffraction study. Am Mineral 80: 197–200

Duffy TS, Zha CS, Downs RT, Mao H, Hemley RJ (1995) Elasticity of forsterite to 16GPa and the composition of the upper mantle. Nature 378: 170–173

Ghose S (1981) Recent trends in the crystal-chemistry of rock forming silicates. Bull Mineral 104: 145–160

Henderson CMB, Knight KS, Redfern SAT, Wood BJ (1995). High-temperature study of octahedral cation exchange in olivine by neutron powder diffraction. Science 271: 1713–1715

Hull S, Smith RI, David WIF, Hannon AC, Mayers J, Cywinski R (1992) The POLARIS powder diffractometer at ISIS. Physica B 180: 1000–1002

Larson AC, Von Dreele RB (1994) GSAS general structure analysis system. LAUR 86-748, Los Alamos National Laboratory, Los Alamos, NM 87545, USA

Jeanloz R (1995) Earth dons a different mantle. Nature 378: 130–131

Oberti R, Ungaretti L, Canillo E, Hawthorne FC, Memmi I (1995) Temperature-dependent Al order-disorder in the tetrahedral double chain of $C2/m$ amphiboles. Eur J Mineral 7: 1049–1063

Redfern SAT, Henderson CMB, Wood BJ, Harrison RJ, Knight KS (1996) Determination of olivine cooling rate from metal-cation ordering. Nature 381: 407–409

Redfern SAT, Henderson CMB, Knight KS, Wood BJ (1997) High-temperature order-disorder in $(Fe_{0.5}Mn_{0.5})_2SiO_4$ and $(Mg_{0.5}Mn_{0.5})_2SiO_4$ olivines: an in situ neutron diffraction study. Eur J Mineral 9: 287–300

Rinaldi R, Wilson CC (1996) Crystal dynamics by neutron time-of-flight Laue diffraction in olivine up to 1573 K using single frame methods. Sol State Commun 97/5: 395–400

Rinaldi R, Artioli G, Wilson CC, McIntyre G (2000) Octahedral cation ordering in olivine at high temperature. I: in situ neutron single-crystal diffraction studies on natural mantle olivines (Fa12 and Fa10). Phys Chem Miner 27: 623–629

Walsh D, Donnay G, Donnay JDH (1974) Jahn-Teller effects in ferro-magnesian minerals. Bull Soc Fr Minéral Cristallogr 97: 170–183